HHS Public Access

Author manuscript

Mol Imaging Biol. Author manuscript; available in PMC 2021 December 01.

Published in final edited form as:

Mol Imaging Biol. 2020 December ; 22(6): 1489–1494. doi:10.1007/s11307-020-01494-9.

Caspase-based PET for Evaluating Pro-Apoptotic Treatments in a Tuberculosis Mouse Model

Alvaro A. Ordonez[1,2], **Sudhanshu Abhishek**[1,2], **Alok K. Singh**[1,2,#], **Mariah H. Klunk**[1,2], **Babak Benham Azad**[3], **Eric O. Aboagye**[4], **Laurence S. Carroll**[1,3,*], **Sanjay K. Jain**[1,2,3,*]

[1]Center for Infection and Inflammation Imaging Research, Johns Hopkins University School of Medicine, Baltimore, MD, USA

[2]Department of Pediatrics, Johns Hopkins University School of Medicine, Baltimore, MD, USA

[3]Russell H. Morgan Department of Radiology and Radiological Sciences, Johns Hopkins University School of Medicine, Baltimore, MD, USA

[4]Comprehensive Cancer Imaging Centre, Department of Surgery & Cancer, Hammersmith Campus, Imperial College, London, UK

Abstract

Purpose—Despite recent advances in antimicrobial treatments, tuberculosis (TB) remains a major global health threat. *Mycobacterium tuberculosis* proliferates in macrophages preventing apoptosis by inducing anti-apoptotic proteins leading to necrosis of the infected cells. Necrosis then leads to increased tissue destruction, reducing the penetration of antimicrobials and immune cells to the areas where they are needed most. Pro-apoptotic drugs could be used as host-directed therapies in TB to improve antimicrobial treatments and patient outcomes.

Procedure—We evaluated [^{18}F]-ICMT-11, a caspase-3/7-specific positron emission tomography (PET) radiotracer, in macrophage cell cultures and in an animal model of pulmonary TB that closely resembles human disease.

Results—Cells infected with *M. tuberculosis* and treated with cisplatin accumulated [^{18}F]-ICMT-11 at significantly higher levels compared to controls, which correlated with levels of caspase-3/7 activity. Infected mice treated with cisplatin with increased caspase-3/7 activity also had a higher [^{18}F]-ICMT-11 PET signal compared to untreated infected animals.

Conclusions—[^{18}F]-ICMT-11 PET could be used as a noninvasive approach to measure intralesional pro-apoptotic responses *in situ* in pulmonary TB models and support the development of pro-apoptotic host-directed therapies for TB.

[*]Co-corresponding authors: Laurence S. Carroll, 720 Rutland Avenue, Ross Research Building Room 320, Baltimore, MD, 21205, USA, lcarro19@jhmi.edu; Phone: 410-619-0109; Sanjay K. Jain, 1550 Orleans St, CRB 2 Room 1.09, Baltimore, MD, 21205, USA, sjain5@jhmi.edu, Phone: 410-502-8241, Fax: 410-614-8173.

[#]Current address: 3 Amity Institute of Biotechnology, Amity University, Noida, Uttar Pradesh, India

Conflict of Interest: None of the authors report any financial or potential conflicts of interest.

Keywords

Tuberculosis; PET; Apoptosis; Caspase; Imaging

Introduction

Tuberculosis (TB) remains one of the top 10 causes of death overall and represents the leading cause of death from a single infectious agent. The World Health Organization estimates that 1.45 million people died due to TB in 2018 [1]. The upsurge of drug-resistance in TB has led to the urgent need of not only expanding the antimicrobial drug pipeline but also evaluating other non-antimicrobial therapeutic strategies that could reduce TB pathology and shorten treatment duration, impede disease transmission, and improve overall health in patients.

During the early phase of infection, *Mycobacterium tuberculosis* proliferates in macrophages, preventing apoptosis by the induction of anti-apoptotic proteins from the Bcl-2 family, leading to necrosis of the infected cells [2–3]. Necrosis increases TB-associated morbidity by causing tissue destruction, promoting fibrosis, and impairing vascular supply, thereby reducing the penetration of antimicrobials and immune cells to the areas where they are needed most [4]. The necrotic centers of granulomas also provide a breeding ground for mycobacterial replication and can transform into cavities, leading to an increased likelihood of developing drug resistance, failing treatment, and transmitting the disease. Conversely, apoptosis serves as a host-protective mechanism by eliminating infected cells without triggering an excessive inflammatory response [2, 5–6].

Recently, there has been an increased interest in developing host-directed therapies (HDTs) that target the host responses to reduce local pathology and shorten TB treatments [7–9]. Pro-apoptotic treatments that modulate the immune response and reduce tissue damage could serve as HDTs in TB. Some novel drugs, like BH3 mimetics that selectively inhibit proteins of the Bcl-2 family, have shown promising results with limited side effects [10]. However, preclinical screening of HDTs in animal models of TB is a cumbersome process with readouts traditionally limited to quantification of the bacterial burden in infected tissues. This approach neither provides insights into disease heterogeneity within the same host, nor does it allow longitudinal evaluations of the same host to detect changes with treatments. We have previously used positron emission tomography (PET) imaging to evaluate the immune response in C3HeB/FeJ mice, which after aerosol infection with *M. tuberculosis*, develops necrotic and hypoxic granulomas closely resembling human pathology, including cavitation [11–12]. In this study, we evaluated a fluorine-18 labeled isatin-containing compound, which is a caspase-3/7-specific PET radiotracer previously validated in oncology [13–14], to detect pro-apoptotic responses in *M. tuberculosis* infection. We used cisplatin-induced apoptosis as a proof-of-concept that [^{18}F]-ICMT-11 PET could be used to monitor the activation of caspase-3/7 in the mouse model of pulmonary TB.

Materials and Methods

All protocols were approved by the Johns Hopkins Biosafety, Radiation Safety, and Animal Care and Use Committees.

Radiosynthesis

[^{18}F]-ICMT-11 was synthesized from the precursor, as previously described (Figure 1) [15]. The radiochemical purity of [^{18}F]-ICMT-11 was >98%, with an average specific activity of 150 ± 5 GBq/μmol.

In vitro assays

Primary peritoneal macrophages were isolated from C3HeB/FeJ mice (Jackson Laboratory) and seeded in a 12-well plate and cultured in RPMI-GlutaMAX (Thermo Fisher Scientific) with 10% heat-inactivated fetal bovine serum at 37°C with 5% CO_2. Once the cell cultures reached 80% confluency, the cells were infected with *M. tuberculosis* H37Rv at a multiplicity of infection (MOI) of 1:5. After two hours, the infected cells were washed with phosphate buffer saline (PBS) and incubated for two additional hours with amikacin (20 μg/ml, Sigma) to eliminate extracellular bacteria. Twenty-four hours post-infection, some of the cells were incubated with cisplatin (200 μM, Sigma) over 12 hours. Next, 0.74 MBq of [^{18}F]-ICMT-11 was added to each well as previously described [16]. After a 60-minute incubation period, cells were detached from the well, (0.25% trypsin; 1 mM EDTA), washed with PBS, lysed (RIPA buffer, Thermo Fisher Scientific) and the associated radioactivity was determined using an automated γ-counter (1282 Compugamma CS Universal γ-counter; LKB Wallac). Uninfected and untreated cells were used as controls. A minimum of four replicates was used for each group, and data are presented as total radioactivity corrected for mg of protein (Bradford Assay; Sigma). To evaluate caspase-3/7 activity, macrophages were infected with *M. tuberculosis* and treated with cisplatin as described above. After 12 hours of incubation with cisplatin (200 μM), the cells were resuspended in cell lysis buffer to measure caspase 3/7 activity using a fluorometric assay (Caspase-3 Assay Kit, ab39383, Abcam) as previously described [17]. After incubation in the cell lysis buffer on ice for 10 minutes, the lysate was transferred into 96-well plates containing the reaction buffer (10 mM dithiothreitol) and 50 μM DEVD-AFC (AFC: 7-amino-4-trifluoromethyl coumarin) as the fluorogenic substrate and incubated at 37°C for 1 hour. Upon cleavage by caspase-3/7, the free AFC emits a yellow-green fluorescence signal that was quantified using a fluorescence plate reader (FLUOstar OPTIMA FL microplate reader, BMG Labtech) with a 400 nm-excitation and 505 nm-emission filter.

Animal infection and treatment

Four- to six-week-old female C3HeB/FeJ mice (Jackson Laboratory) were aerosol-infected with *M. tuberculosis* H37Rv using the Middlebrook Inhalation Exposure System (Glas-Col) with frozen titrated bacterial stocks as previously described [12]. Mice were sacrificed to determine the pulmonary bacillary burden as colony-forming units (CFU) one day after infection and at the imaging time point, as described previously [11–12]. At least three mice were used for each group per time point.

Imaging

After an incubation period of 12 weeks post-infection, the *M. tuberculosis*-infected animals were randomly assigned to a treatment group that received a single dose of cisplatin (15 mg/kg, Sigma) intraperitoneally, and a control group that was similarly treated with PBS. Six hours later, the mice received 4.83 ± 0.60 MBq of [^{18}F]-ICMT-11 via tail vein and were imaged within a sealed biocontainment bed (Minerve), as described previously [18]. Dynamic PET was acquired from 15 to 60 minutes post-injection (nanoScan PET/CT, Mediso) and reconstructed into 5-minute frames. Next, a computed tomography (CT) was acquired for anatomical coregistration. Scatter and attenuation correction were applied to the PET data, which was visualized using VivoQuant 4.0 (Invicro). Quantification of the [^{18}F]-ICMT-11 activity in tissues was performed by drawing volumes of interest (VOIs) on the pulmonary affected areas, based on the CT, using AMIDE 1.0.4. Data for blood activities were obtained by placing a VOI in the left ventricle of the heart. The PET data are expressed as % injected dose (ID) per volume of tissue (mL).

Measurement of caspase-3/7 activity in mouse lungs

A similar *M. tuberculosis*-infected cohort of mice was treated with a single dose of cisplatin (15 mg/kg) as described above. Six hours later, the animals were sacrificed under anesthesia. Lung tissues were harvested and processed for protein isolation using RIPA buffer (Sigma). Caspase-3/7 activity was quantified using the Caspase-Glo® 3/7 assay kit (no. G8090, Promega) according to the manufacturer's protocol. An equal amount of protein (50 μg) was incubated with the luminogenic caspase-3/7 substrate (DEVD) at a ratio of 1:1. As described above, the associated luminescence signal was quantified using a plate reader. Healthy and untreated mice were used as controls. At least three mice were used in each experimental group.

Statistical analysis

Statistical comparisons for *in vitro* data and the *in vivo* caspase-3/7 activity data were performed using an unpaired two-tailed Student's t test (Prism 8.3.1, GraphPad Software), while a two-tailed Mann-Whitney *U* test was used for the imaging data. Differences between groups were considered significant if $P \leq 0.05$.

Results

The radiosynthesis of [^{18}F]-ICMT-11 was performed under modified conditions compared to previous literature reports [15], consisting of using a different synthetic box (an Elixys FLEX/CHEM versus a GE FASTLab), with a series of associated minor alterations (e.g. volumes used), but with minimal disturbance to the radiochemical yield or purity. The acetal-protected tosylate precursor **1** was labeled using standard S_N2 radiolabeling conditions, followed by acid-mediated deprotection and semi-preparative HPLC purification, leading to a 12 ± 2 % non-decay corrected radiochemical yield (n = 7).

Cellular uptake of [^{18}F]-ICMT-11 correlated well with the proportion of cisplatin-induced apoptosis (Figure 2a). Untreated infected and uninfected cells had a similarly low accumulation of [^{18}F]-ICMT-11 ($P = 0.21$). Conversely, uninfected cells treated with

cisplatin had a significant increase in tracer accumulation ($P < 0.001$). *M. tuberculosis*-infected cells treated with cisplatin had significantly higher uptake of [^{18}F]-ICMT-11 compared to infected untreated cells ($P = 0.001$), but lower compared to the uninfected treated cells ($P < 0.001$). These findings correlated with the observed *in vitro* caspase-3/7 activity. Cisplatin treatment induced a significantly higher caspase-3/7 activity in both uninfected ($P < 0.0001$) and *M. tuberculosis*-infected cells ($P = 0.028$) (Figure 2b).

We next evaluated the ability of [^{18}F]-ICMT-11 PET to detect differences associated with cisplatin treatment within the affected lung areas of *M. tuberculosis*-infected mice. At the time of imaging, the bacterial burden in the lungs of the infected mice was 7.68 ± 0.31 $\log_{10}$ CFU/mL. Uninfected mice and infected treated with cisplatin had higher caspase-3/7 activity in lung tissues compared to cisplatin-naïve animals ($P < 0.05$) (Figure 3a). Infection with *M. tuberculosis* reduced the caspase-3/7 activity in lung tissues, likely due to the mycobacterial induction of anti-apoptotic proteins [2–3]. After injection, most of the [^{18}F]-ICMT-11 PET rapidly distributed among all tissues, including the hepatobiliary tract and lungs (Figures 3b–d). While the [^{18}F]-ICMT-11 activity in the blood of both the cisplatin-treated and control groups was similar (Figure 4a), the activity in the affected lung areas was higher in mice that received cisplatin (Figure 4b). [^{18}F]-ICMT-11 PET was able to detect the increased pro-apoptotic response in the affected lung areas with an area under the curve for 30 to 60 minutes ($AUC_{30–60min}$) 1.4 times higher compared to the affected lung in the control animals ($P < 0.001$, Figure 4c).

Discussion

The pathologic hallmark of TB is the formation of a caseating granuloma, which is composed of a core of necrotic debris surrounded by layers of heterogeneous inflammatory cells contained within a fibrotic capsule [12]. Necrotic debris provides a rich media for bacterial growth and doubles as a barrier to prevent the penetration of antimicrobials and immune cells, contributing to antimicrobial resistance and treatment failure [19]. Necrotic cell death is also pro-inflammatory, releasing numerous chemical mediators that stimulate additional inflammation [20], which could worsen TB pathology. This over-amplification of host responses causes the bulk of TB-associated morbidity and pathology in the lungs [21]. Additionally, necrosis is a prerequisite for the development of pulmonary cavities, leading to the emergence of drug-resistant TB strains, person-to-person transmission, and treatment failure [22]. Necrosis was thought to be a disordered, unregulated, and unavoidable consequence of active infection, but recent studies suggest that *M. tuberculosis* manipulates the host cell to induce necrosis by preventing apoptosis [23]. Therefore, modulating the immune response by promoting pro-apoptosis pathways could be used as HDTs in TB.

[^{18}F]-ICMT-11 is an activated caspase-3/7-specific PET radiotracer previously utilized to monitor apoptosis in tumors [24]. Caspase-3/7 was identified as the ideal target due to their role as effector caspases, given that their activation is the final step prior to cell death, regardless of the source of the initial stimuli that triggered the apoptotic response [25]. [^{18}F]-ICMT-11 has the advantages of being a small molecule with rapid biodistribution and clearance from tissues [26], and high specificity for apoptosis since it does not accumulate in areas of necrosis [16]. The tissue biodistribution of [^{18}F]-ICMT-11 has been previously

described in both mouse models and healthy human subjects [27–29]. Prior studies have used [^{18}F]-ICMT-11 to monitor the pro-apoptotic response in animal models treated with carboplatin and cyclophosphamide with promising results [16, 26]. These findings also reported a low background in the lungs, which would allow the detection of small changes associated with a drug-induced pro-apoptotic response in pulmonary TB. [^{18}F]-ICMT-11 PET was safe, well-tolerated, had favorable dosimetry in healthy volunteers and was recently used to evaluate chemotherapy-induced caspase-3/7 activation in breast and lung cancer patients [14, 29].

We have successfully adapted the radiosynthesis of [^{18}F]-ICMT-11 to evaluate the pro-apoptotic response in cells and mice infected with *M. tuberculosis* and treated with cisplatin. The [^{18}F]-ICMT-11 signal was significantly higher when cell death was induced with cisplatin treatment, which correlated with increased caspase-3/7 activity. Both cells and animals infected with *M. tuberculosis* had a lower caspase-3/7 activity and corresponding ^{18}F-ICMT-11 signal compared to uninfected controls. This is likely due to the known induction of anti-apoptotic proteins by mycobacteria [2–3]. However, ^{18}F-ICMT-11 was able to quantify the increase in the pro-apoptotic response induced by cisplatin in both *M. tuberculosis*-infected cells and mice. In this study, we used cisplatin chemotherapy as a proof-of-concept to observe if [^{18}F]-ICMT-11 PET could monitor the activation of caspase-3/7 in animal models of pulmonary TB. DNA damage induced by cisplatin is known to induce apoptosis in most tissues, leading to significant side effects, including myelosuppression, nephrotoxicity, and peripheral neuropathy [30]. Therefore, cisplatin is not going to be evaluated as a HDT in TB. The use of [^{18}F]-ICMT-11 PET in conjunction with anatomical imaging (e.g., CT, MRI) will allow spatial monitoring of the pro-apoptotic response in affected areas. Our data suggest that [^{18}F]-ICMT-11 PET could be a valuable tool to streamline the evaluation of other possible clinically relevant and safer pro-apoptotic agents, such as the BH3 mimetics, as HDTs in pulmonary TB.

Conclusion

[^{18}F]-ICMT-11 PET can be used as a noninvasive approach to monitor the intralesional pro-apoptotic response in a pulmonary TB mouse model and support the development of pro-apoptotic host-directed therapies for TB.

Acknowledgments

This study was funded by the National Institutes of Health Director's Transformative Research Award R01-EB020539 (SKJ). The funders had no role in study design, data collection, and analysis, decision to publish, or preparation of the manuscript.

References

1. World Health Organization (2019) Global Tuberculosis Report. Geneva, Switzerland: WHO
2. Sly LM, Hingley-Wilson SM, Reiner NE, McMaster WR (2003) Survival of Mycobacterium tuberculosis in host macrophages involves resistance to apoptosis dependent upon induction of antiapoptotic Bcl-2 family member Mcl-1. J Immunol 170:430–437 [PubMed: 12496428]
3. Gan H, Lee J, Ren F, Chen M, Kornfeld H, Remold HG (2008) Mycobacterium tuberculosis blocks crosslinking of annexin-1 and apoptotic envelope formation on infected macrophages to maintain virulence. Nat Immunol 9:1189–1197 [PubMed: 18794848]

4. Ordonez AA, Wang H, Magombedze G, et al. (2020) Dynamic imaging in Tuberculosis patients reveals heterogeneous drug exposures in pulmonary lesions. Nat Med. 10.1038/s41591-020-0770-2
5. Wang Q, Liu S, Tang Y, Liu Q, Yao Y (2014) MPT64 protein from Mycobacterium tuberculosis inhibits apoptosis of macrophages through NF-kB-miRNA21-Bcl-2 pathway. PloS One 9:e100949 [PubMed: 25000291]
6. Zhao X, Khan N, Gan H, et al. (2017) Bcl-xL mediates RIPK3-dependent necrosis in M. tuberculosis-infected macrophages. Mucosal Immunol 10:1553–1568 [PubMed: 28401933]
7. Ordonez AA, Maiga M, Gupta S, Weinstein E, Bishai WR, Jain SK (2014) Novel adjunctive therapies for the treatment of tuberculosis. Curr Mol Med 14:385–395 [PubMed: 24236454]
8. Ordonez AA, Pokkali S, Kim S, et al. (2018) Adjunct antibody administration with standard treatment reduces relapse rates in a murine tuberculosis model of necrotic granulomas. PLoS One 13:e0197474. [PubMed: 29758082]
9. Ordonez AA, Pokkali S, Sanchez-Bautista J, et al. (2019) Matrix metalloproteinase inhibition in a murine model of cavitary tuberculosis paradoxically worsens pathology. J Infect Dis 219:633–636 [PubMed: 29920600]
10. Singh R, Letai A, Sarosiek K (2019) Regulation of apoptosis in health and disease: the balancing act of BCL-2 family proteins. Nat Rev Mol Cell Biol 20:175–193 [PubMed: 30655609]
11. Ordonez AA, Pokkali S, DeMarco VP, et al. (2015) Radioiodinated DPA-713 imaging correlates with bactericidal activity of tuberculosis treatments in mice. Antimicrob Agents Chemother 59:642–649 [PubMed: 25403669]
12. Ordonez AA, Tasneen R, Pokkali S, et al. (2016) Mouse model of pulmonary cavitary tuberculosis and expression of matrix metalloproteinase-9. Dis Model Mech 9:779–788. [PubMed: 27482816]
13. Nguyen Q-D, Smith G, Glaser M, Perumal M, Årstad E, Aboagye EO (2009) Positron emission tomography imaging of drug-induced tumor apoptosis with a caspase-3/7 specific [^{18}F]-labeled isatin sulfonamide. Proc Natl Acad Sci USA 106:16375–16380 [PubMed: 19805307]
14. Dubash SR, Merchant S, Heinzmann K, et al. (2018) Clinical translation of [^{18}F]ICMT-11 for measuring chemotherapy-induced caspase 3/7 activation in breast and lung cancer. Eur J Nucl Med Mol Imaging 45:2285–2299 [PubMed: 30259091]
15. Fortt R, Smith G, Awais RO, Luthra SK, Aboagye EO (2012) Automated GMP synthesis of [^{18}F] ICMT-11 for in vivo imaging of caspase-3 activity. Nucl Med Biol 39:1000–1005 [PubMed: 22575271]
16. Witney TH, Fortt RR, Aboagye EO (2014) Preclinical assessment of carboplatin treatment efficacy in lung cancer by 18F-ICMT-11-positron emission tomography. PLoS One 9:e91694 [PubMed: 24618809]
17. Yang M, Chen P, Liu J, et al. (2019) Clockophagy is a novel selective autophagy process favoring ferroptosis. Sci Adv 5:eaaw2238 [PubMed: 31355331]
18. Weinstein E, Liu L, Ordonez A, et al. (2012) Noninvasive determination of 2-[18F]-fluoroisonicotinic acid hydrazide pharmacokinetics by positron emission tomography in Mycobacterium tuberculosis-infected mice. Antimicrob Agents Chemother 56:6284–6290 [PubMed: 23006755]
19. Prideaux B, Via LE, Zimmerman MD, et al. (2015) The association between sterilizing activity and drug distribution into tuberculosis lesions. Nat Med 21:1223–1227 [PubMed: 26343800]
20. Kaczmarek A, Vandenabeele P, Krysko DV (2013) Necroptosis: the release of damage-associated molecular patterns and its physiological relevance. Immunity 38:209–223 [PubMed: 23438821]
21. Ernst JD (2012) The immunological life cycle of tuberculosis. Nat Rev Immunol 12:581–591 [PubMed: 22790178]
22. Perrin FM, Woodward N, Phillips PP, et al. (2010) Radiological cavitation, sputum mycobacterial load and treatment response in pulmonary tuberculosis. Int J Tuberc Lung Dis 14:1596–1602 [PubMed: 21144246]
23. Torrado E, Robinson RT, Cooper AM (2011) Cellular response to mycobacteria: balancing protection and pathology. Trends Immunol 32:66–72 [PubMed: 21216195]
24. Nguyen Q-D, Challapalli A, Smith G, Fortt R, Aboagye EO (2012) Imaging apoptosis with positron emission tomography:'bench to bedside'development of the caspase-3/7 specific radiotracer [^{18}F] ICMT-11. Eur J Cancer 48:432–440 [PubMed: 22226480]

25. Taylor RC, Cullen SP, Martin SJ (2008) Apoptosis: controlled demolition at the cellular level. Nat Rev Mol Cell Biol 9:231–241 [PubMed: 18073771]

26. Nguyen Q-D, Lavdas I, Gubbins J, et al. (2013) Temporal and spatial evolution of therapy-induced tumor apoptosis detected by caspase-3–selective molecular imaging. Clin Cancer Res 19:3914–3924 [PubMed: 23729364]

27. Smith G, Glaser M, Perumal M, et al. (2008) Design, synthesis, and biological characterization of a caspase 3/7 selective isatin labeled with 2-[^{18}F]fluoroethylazide. J Med Chem 51:8057–8067 [PubMed: 19049429]

28. Vassileva V, Stribbling SM, Barnes C, et al. (2019) Evaluation of apoptosis imaging biomarkers in a genetic model of cell death. EJNMMI Res 9:18 [PubMed: 30783791]

29. Challapalli A, Kenny LM, Hallett WA, et al. (2013) 18F-ICMT-11, a caspase-3–specific PET tracer for apoptosis: biodistribution and radiation dosimetry. J Nucl Med 54:1551–1556 [PubMed: 23949910]

30. Fisher DE (1994) Apoptosis in cancer therapy: crossing the threshold. Cell 78:539–542. [PubMed: 8069905]

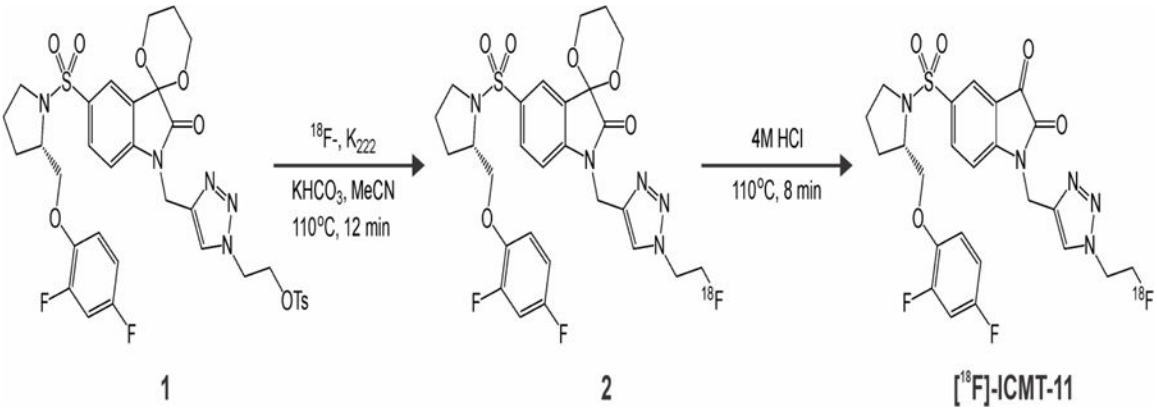

Figure 1.
Radiolabeling of [^{18}F]-ICMT-11.

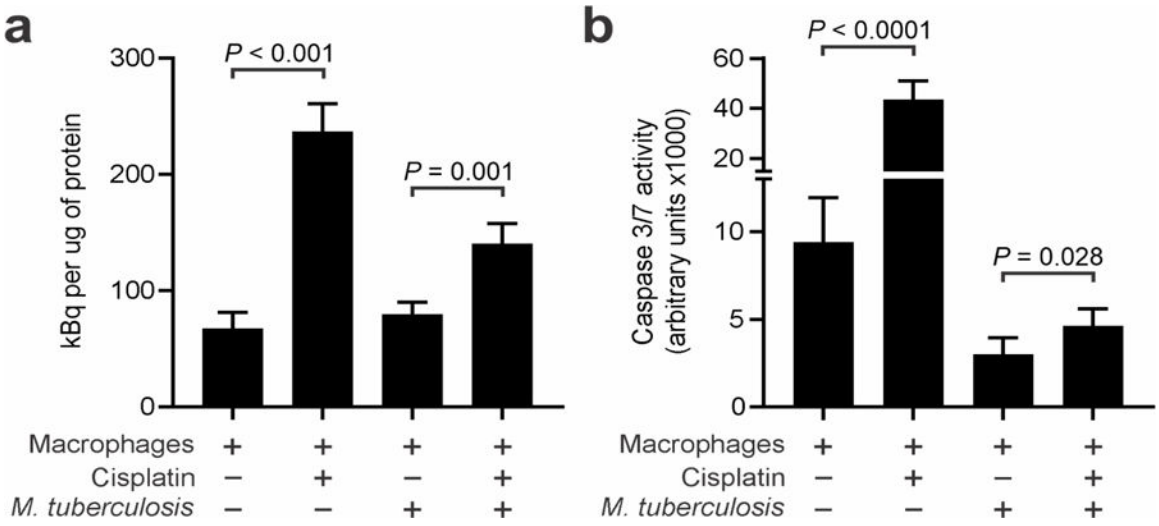

Figure 2.

To determine the *in vitro* accumulation of [^{18}F]-ICMT-11, macrophages were infected with *M. tuberculosis* and exposed to cisplatin. (**a**) The uninfected cisplatin-treated cells had a higher accumulation of [^{18}F]-ICMT-11 over a 60-minute incubation period. *M. tuberculosis*-infected cells treated with cisplatin also had a higher tracer accumulation compared to untreated cells. (**b**) Caspase-3/7 activity was also determined in these cells by using a fluorometric assay. Data represented as mean and standard deviation.

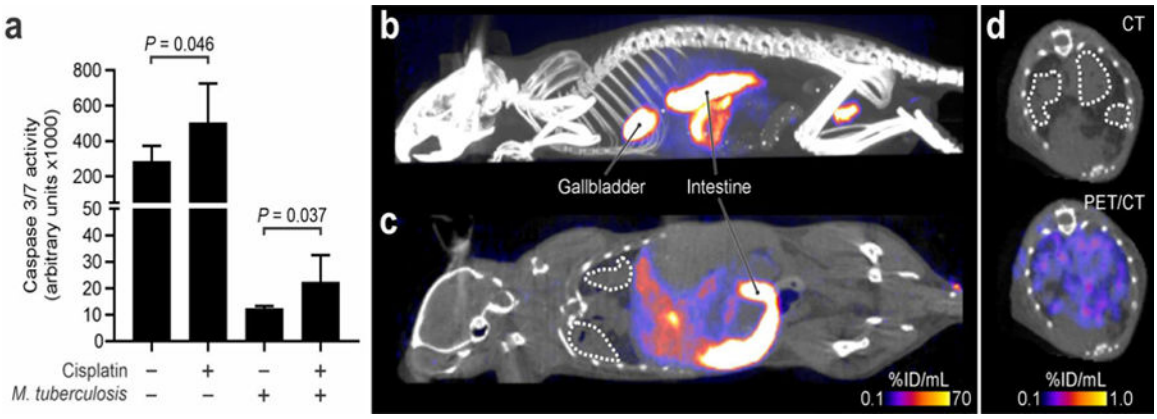

Figure 3.

(**a**) Caspase-3/7 activity in mouse lungs. At least two replicates for three mice per group were used. Data represented as mean and standard deviation. Maximum intensity projection (**a**) and coronal section (**b**) of the [^{18}F]-ICMT-11 PET/CT in *M. tuberculosis*-infected mice 20 minutes post-injection in a representative cisplatin-treated mouse. (**d**) Transverse section of the CT and [^{18}F]-ICMT-11 PET/CT from the same mouse as panels b and c. The affected lung areas are marked by dotted white lines.

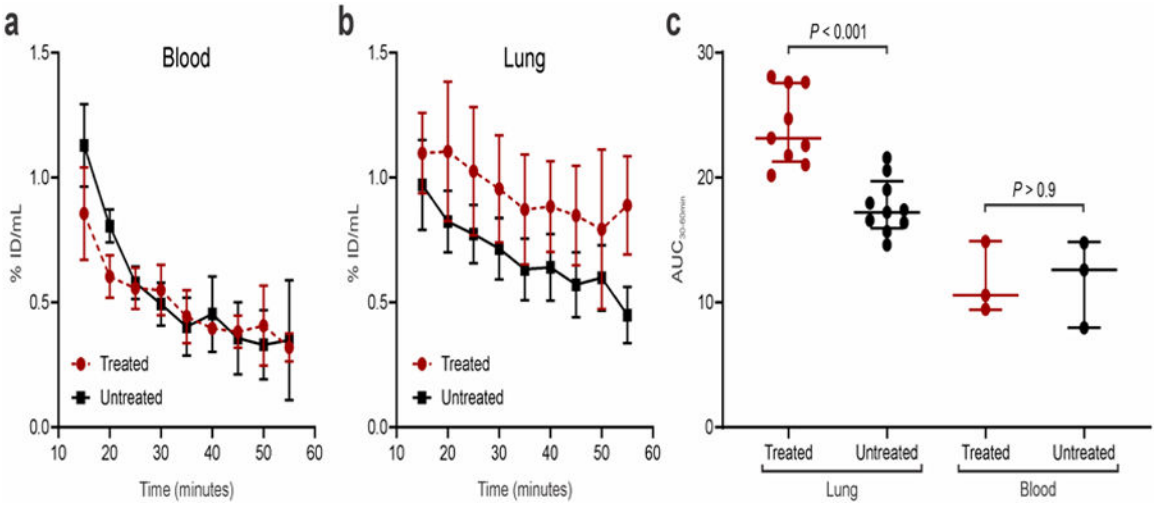

Figure 4.

[^{18}F]-ICMT-11 PET in *M. tuberculosis*-infected mice. (**a**) The time-activity curve for [^{18}F]-ICMT-11 in the blood showed no differences between cisplatin-treated and untreated mice. (**b**) The time-activity curve in the affected areas of the lung showed increased [^{18}F]-ICMT-11 PET signal in the cisplatin-treated animals. (**c**) The area under the curve (AUC) for 30–60 minutes post-injection showed a significantly higher signal in the lungs of cisplatin-treated animals compared to untreated controls ($P < 0.001$). Conversely, there were no differences in the blood ($P > 0.9$). Data represented as median and interquartile ranges.